Journal of Catalysis 281 (2011) 318–324

Contents lists available at ScienceDirect

Journal of Catalysis

journal homepage: www.elsevier.com/locate/jcat

Photocatalytic H_2 production on hybrid catalyst system composed of inorganic semiconductor and cobaloximes catalysts

Fuyu Wen [a,b], Jinhui Yang [a,b], Xu Zong [a], Baojun Ma [a], Donge Wang [a,b], Can Li [a,*]

[a] State Key Laboratory of Catalysis, Dalian National Laboratory for Clean Energy, Dalian Institute of Chemical Physics, Chinese Academy of Sciences, Dalian 116023, China
[b] Graduate University of Chinese Academy of Sciences, Beijing 100049, China

ARTICLE INFO

Article history:
Received 20 January 2011
Revised 25 March 2011
Accepted 12 May 2011
Available online 17 June 2011

Keywords:
Photocatalysis
Hydrogen
Hybrid system
Semiconductor
Cobaloximes catalysts

ABSTRACT

An artificial photocatalytic system mimicking photosystem I (PSI) has been assembled using semiconductor (CdS) as photosensitizer, cobaloximes (Co^{III} complexes) as H_2 evolution catalysts, and triethanolamine (TEOA) as sacrificial electron donor. This artificial photocatalytic system shows high hydrogen evolution activity (turnover number up to 171 based on $Co^{III}(dmgH)_2pyCl$ **1**) under visible light irradiation. The apparent quantum efficiency (QE) for **1**/CdS hybrid photocatalytic system in acetonitrile solution at 420 nm is calculated to be 9.1%. The interfacial electron transfer from photoexcited CdS to Co^{III} complexes is very efficient through the weak adsorption of Co^{III} complexes on CdS. The adsorption of **1** on CdS in acetonitrile fits Langmuir equation, the maximum monolayer adsorption capacity is 3×10^{-3} mmol g^{-1}, which means most of **1** are in the solution. The rate of hydrogen production exhibits a quadratic dependence on the total concentration of **1**. Therefore, a bimetallic catalysis pathway is proposed. The efficient electron transfer, the broad electronic absorption character of CdS photosensitizer as well as the H_2 evolution ability of Co^{III} complexes, account for the high photocatalytic activity of this hybrid photocatalytic system.

1. Introduction

Artificial photosynthetic H_2 evolution which converts solar energy into chemical fuel has been attracting much attention as one of the promising strategies to provide clean energy for the future [1,2]. Many homogeneous electrocatalytic H_2 evolution systems based on biomimetic hydrogenases have been developed [3–9]. For homogeneous photocatalysis, photosensitizers are usually integrated with biomimetic hydrogenases [10–12]. Na et al. constructed a three components system which consisted of in situ reduced $Ru(bpy)_3^+$ as photosensitizer, bioinspired $[Fe_2S_2]$ model complex as H_2 evolution catalyst, and diethyldithiocarbamate anion (dtc^-) as sacrificial electron donor [13]. Visible light driven hydrogen evolution was successfully realized in this three-component system [14]. Besides $[Fe_2S_2]$ complexes, cobaloximes which possess high electrocatalytic hydrogen evolution activity were also widely studied as functional models of hydrogenases [15–23]. Fihri et al. reported that cobaloxime complexes covalently linked with photosensitizers such as $[(bpy)_2Ru(L\text{-}pyr)]^{2+}$, $[(ppy)_2Ir(L\text{-}pyr)]^+$ can also drive photocatalytic H_2 evolution through intramolecular electron transfer [24,25]. When cobaloximes were just mechanically mixed with Pt, Re complexes or Eosin Y photosensitizers in aqueous solutions, photocatalytic hydrogen evolution can also be achieved through the intermolecular electron transfer [26–31].

In the systems mentioned previously, photosensitizers are the organometallic complexes or organic compounds. However, this type of photosensitizers can only absorb a light of particular wavelength or a narrow region of light, and furthermore suffer the problem of instability or even degradation under photoirradiation condition [29]. On the other hand, the spectral absorption range of semiconductors is usually broad and continuous, and this is potentially beneficial for the efficient collection of solar energy [32–36]. When semiconductors are excited by photons with energy larger than the band gap of semiconductors (Eg), electron/hole pairs can also be generated just similar to the processes in organometallic complex photosensitizers [32]. Using semiconductor to replace the traditional organometallic complexes as photosensitizer may overcome the drawbacks of narrow spectral absorption and poor stability of the organometallic complex photosensitizers [37].

Herein, we report an inexpensive and stable artificial photocatalytic system to mimic photosystem I (PSI) using semiconductor (CdS) as photosensitizer, cobaloximes (Co^{III} complexes) as the catalysts for H_2 evolution, and triethanolamine (TEOA) as sacrificial reducing agent. Under visible light irradiation ($\lambda > 420$ nm), photocatalytic H_2 evolution with more than 171 turnover numbers (based on $Co^{III}(dmgH)_2pyCl$ **1**) can be achieved, which is comparable with the highest TON obtained from homogeneous Co

* Corresponding author. Fax: +86 411 84694447.
E-mail address: canli@dicp.ac.cn (C. Li).
URL: http://www.canli.dicp.ac.cn (C. Li).

0021-9517/$ - see front matter © 2011 Elsevier Inc. All rights reserved.
doi:10.1016/j.jcat.2011.05.015

complexes-based photocatalytic systems [25–27]. The rate of H_2 evolution catalyzed by this hybrid system is 26 times higher than that catalyzed by CdS alone under the same experimental conditions. The present work demonstrates the feasibility of using semiconductors as photosensitizers and cobaloximes complexes as H_2 evolution catalysts.

2. Experimental

2.1. Preparation of CdS and Cobalt complexes

All of the reagents were of analytical grade and were used without further purification. The CdS nanoparticles were prepared by a precipitation-hydrothermal process [36]. An aqueous solution of Na_2S (800 mL, 0.14 mol L^{-1}) was added slowly to $Cd(OAc)_2$ solution (1000 mL, 0.14 mol L^{-1}) under vigorous stirring. The yellow mixture was stirred for 24 h and kept for an additional 24 h. The resulting yellow slurry was filtered. The wet solid was suspended in pure water (120 mL) and transferred to a Teflon-lined stainless steel autoclave (150 mL) and heated at 250 °C for 24 h (hydrothermal treatment). The yellow solid was filtered, washed with water and ethanol subsequently, and dried under vacuum at 95 °C for 24 h.

$Co^{III}(dmgH)_2pyCl$ **1** was synthesized according to the literature [38]. To a hot solution (70 °C) of 2.5 g (0.0105 mol) of $CoCl_2{\cdot}6H_2O$, 2.75 g (0.0235 mol) of dimethylglyoxime (dmgH), and 0.42 g (0.0105 mol) of NaOH in 100 ml of 95% ethanol, 0.86 g (0.0105 mol) of pyridine was added under N_2 atmosphere. After cooling to 20 °C, a stream of air was blown through the solution for 30 min. The reaction mixture was then allowed to stand for 60 min at 20 °C, during which period the product was crystallized out of the solution. The brown crystals were collected by filtration, washed successively with water, ethanol, and diethyl ether, and extracted with acetone. Removal of the solvent from the extracts yielded pure **1** (2.14 g, 53.5%). Anal. Calcd. for $C_{13}H_{19}N_5O_4ClCo$: C, 38.67; H, 4.74; N, 17.35. Found: C, 39.10; H, 4.83; N, 17.62. ^1H NMR (400 MHz, DMSO-d6): δ (ppm) = 8.03, 8.04 (2H, Pyridine-αH); 7.87, 7.89, 7.91 (1H, Pyridine-γH); 7.47, 7.48, 7.45 (2H, Pyridine-βH); 2.27 (12H, dimethylglyoxime).

$Co^{III}(dmgH)_2$(4-(Me_2N)py)Cl **2** was synthesized according to the literature [21]. $CoCl_2{\cdot}6H_2O$ (2.5 g, 0.0105 mol), dimethylglyoxime (2.75 g, 0.0235 mol), and NaOH (0.42 g, 0.0105 mol) were dissolved in 95% ethanol (100 mL) and heated to 70 °C under N_2 atmosphere. 4-(Dimethylamino) pyridine (1.315 g, 10.5 mmol) was then added, and the resulting solution was cooled to room temperature. A stream of air was then passed through the solution for 30 min, which caused precipitation of a brown solid. The suspension was stirred for 1 h and filtered. The precipitate was successively washed with water, ethanol, and diethyl ether. The product was then extracted with acetone. Removal of the solvent from the extracts yielded pure **2** (1.937 g, 40%). Anal. Calcd. for $C_{15}H_{24}N_6O_4ClCo$: C, 40.32; H, 5.41; N, 18.81. Found: C, 41.61; H, 5.62; N, 17.91. ^1H NMR (400 MHz, DMSO-d6) of **2**: δ (ppm) = 7.36, 7.35 (2H, Pyridine); 6.58, 6.57 (2H, Pyridine); 2.90 (6H, NMe_2); 2.30 (12H, dimethylglyoxime).

$Co^{III}(dmgH)_2$(2-(SH)py)Cl **3** was synthesized similar to literature [39]. $CoCl_2{\cdot}6H_2O$ (1.19 g, 5 mmol) and dimethylglyoxime (1.16 g, 10 mmol) were dissolved in 95% ethanol (150 mL) and heated to 70 °C under N_2 atmosphere. 2-Mercaptopyridine (1.11 g, 10 mmol) was then added, and the resulting solution was cooled to room temperature. A stream of air was then passed through the solution for 30 min, which caused precipitation of a brown solid. The suspension was stirred for 1 h and filtered. The precipitate was successively washed with water, ethanol, and diethyl ether. The product was then extracted with acetone. Removal of the solvent from the extracts yielded pure **3** (0.89 g, 41%). Anal. Calcd. for $C_{13}H_{19}N_5O_4ClCo$: C, 38.70; H, 4.71; N, 17.37. Found: C, 39.20; H, 4.81; N, 17.58. ^1H NMR (400 MHz, DMSO-d6) of **3**: δ (ppm) = 8.37 (1H, Pyridine); 8.13(1H, Pyridine); 7.74 (1H, Pyridine); 7.36 (1H, Pyridine); 2.28 (12H, dimethylglyoxime).

2.2. Characterization

Cyclic voltammograms were recorded on a BAS-100B electrochemical potentiostat using a three electrode cell at a scan rate of 100 mV S^{-1} under argon atmosphere. The working electrode was a glass carbon disk (0.071 cm^2) polished with 3 and 1 μm diamond pastes and sonicated in deionized water bath for 10 min prior to use. The reference electrode was Ag/Ag^+ (0.01 M $AgNO_3$) in CH_3CN, and the auxiliary electrode was a platinum wire. The DMF (Aldrich, spectroscopy grade) used for electrochemical measurements was freshly dried over calcium hydride prior to use. A solution of 0.1 M nBu_4NPF_6 (Fluka, electrochemical grade) in DMF was used as electrolyte. All redox potentials were measured relative to the ferrocenium/ferrocene (Fc^+/Fc) couple and then adjusted to NHE.

The amount of Co^{III} complexes adsorbed to CdS was obtained by subtracting the value obtained from the original and equilibrium concentration by using the relation (1) [40]:

$$C_s = (C_0 - C_e) \times V_s/m \tag{1}$$

where C_s is the amount adsorbed (mg g^{-1}), C_e is the equilibrium concentration of Co^{III} complexes after adsorption (mg L^{-1}), C_0 is the original concentration of Co^{III} complexes before adsorption (mg L^{-1}), V_s is the solution volume (L), and m is the CdS mass (g). The concentration was determined by UV–Vis absorbance.

Adsorption data were fitted to the Freundlich model (3) or Langmuir model (4):

$$C_s = K_f C_e^{1/n} \tag{2}$$

or the logarithmic form:

$$\log C_s = \log K_f + (1/n)\log C_e \tag{3}$$

where K_f represents the Freundlich adsorption coefficient and gives an estimate of the adsorptive capacity, and $1/n$ describes the isotherm curvature and gives an estimate of the adsorptive intensity.

$$C_e/C_s = C_e/C_m + 1/(bC_m) \tag{4}$$

where C_m is maximum monolayer adsorption capacity (mg g^{-1}), and b is adsorption constant.

The photocatalytic reactions were carried out in a Pyrex reaction cell connected to a closed gas circulation and evacuation system. Hundred ml of 8:1:1 DMF or acetonitrile/H_2O/TEOA solution containing different amounts of Co^{III} complexes and CdS was used in the reactions. The reaction solution was thoroughly degassed and then irradiated by a Xe lamp (300 W) equipped with an optical filter ($\lambda > 420$ nm) to cutoff the light in the ultraviolet region. The amount of H_2 evolved was analyzed using an on-line gas chromatography (Shimadazu; GC-8A, MS-5A column, TCD, Ar Carrier).

The apparent quantum efficiency (QE) was measured under the same photocatalytic reaction condition with irradiation light at 420 nm by using combined band-pass (Kenko) and cutoff filters L38 (HOYA) and 300 W Xe lamp, and the QE was calculated according to Eq. (5):

$$\begin{aligned} \mathrm{QE}\ (\%) &= (\text{number of reacted electrons}/ \\ &\quad \text{number of incident photons}) \times 100 \\ &= (\text{number of evolved } H_2 \text{ molecules} \times 2/ \\ &\quad \text{number of incident photons}) \times 100 \end{aligned} \tag{5}$$

The number of incident photons was 5.32×10^{20} photons h^{-1}, which was measured by using a calibrated Si photodiode (HAMAMATSU S2281). The number of incident photons was also calibrated with ferrioxalate solution in the same device [41].

The TON was calculated according to Eq. (6):

$$\begin{aligned}\mathrm{TON} &= \text{number of product molecules}/\\ &\quad \text{number of catalyst molecules}\\ &= \text{number of evolved}H_2\text{molecules}/\\ &\quad \text{number of catalyst molecules}\end{aligned} \tag{6}$$

3. Results and discussion

CdS nanoparticles with an average diameter of 50 nm, hexagonal structures (Fig. S1) were prepared by a precipitation-hydrothermal process [36]. Co^{III} complexes **1–3** were synthesized according to literatures [21,38,39], and the structures were confirmed by IR, ^1H NMR (Fig. S2, S3), and elemental analysis, as shown in Fig. 1. Cobaloxime/CdS hybrid system was formed by adding CdS nanoparticles into a dilute (e.g., 0.25 mmol L^{-1}) Cobaloxime/dimethyl formamide (DMF) or acetonitrile solution. The combination of cobaloxime with CdS was through adsorption. As shown in Fig. 2, the adsorption data at the range of the concentration of **3** studied can be well described by the Freundlich equation. The calculated adsorption coefficients of **3** on CdS in DMF and acetonitrile are 0.248 and 1.68, respectively. The adsorption of **2** on CdS in acetonitrile also fits Freundlich equation well, the calculated adsorption coefficients is 0.126. The adsorption of **1** on CdS in acetonitrile fits Langmuir equation, the maximum monolayer adsorption capacity is 3×10^{-3} mmol g^{-1}. Given all of the concentration of Co^{III} complexes are 0.25 mmol L^{-1} (100 mL acetonitrile solution), and the mass of CdS is 0.05 g, the adsorption amount of Co^{III} complexes on CdS are 1.43×10^{-2} mmol, 3.06×10^{-3} mmol, and 1.5×10^{-4} mmol for complex **3**, **2,** and **1,** respectively. For complex **1** and **2**, most of the catalysts are in the solution, while 57% of complex **3** are on the surface of CdS. The sequence of the adsorption capacity for Co^{III} complexes on CdS is **3 > 2 > 1.** UV–Vis spectra in Fig. 3 show that CdS can broadly and intensely absorb light from UV to visible region, while **1** only exhibits absorbance in UV region.

The photocatalytic activities of H_2 evolution over CdS and **1**/CdS hybrid system in DMF solvent (line a and b) and over **1**/CdS in acetonitrile solvent (line c) are shown in Fig. 4. In DMF solvent, CdS alone shows low photocatalytic activity (4.4 μmol h^{-1}), corresponding to a QE of 0.08% at 420 nm. When **1** (0.25 mmol L^{-1}) is added, the rate of H_2 evolution is enormously increased up to 26 times (115.0 μmol h^{-1}) and a turnover of 28 is obtained (QE: 2.1% at 420 nm). If acetonitrile is used as the solvent instead of DMF, the photocatalytic activity of this hybrid system can be further enhanced up to 945.6 μmol h^{-1}, corresponding to a QE of 9.1% at 420 nm. A turnover number of 121 (based on **1**) in 6 h is obtained under the same experimental conditions. The increase in photocatalytic activity for the hybrid photocatalysts in acetonitrile may be attributable to the lower reduction potential of **1** in acetonitrile than that in DMF [22] (about 0.1 V in difference) when the disparity in dielectric constants for acetonitrile and DMF is neglectable (36.6 and 38.3 for acetonitrile and DMF, respectively). The presence of water can facilitate the charge separation (dielectric

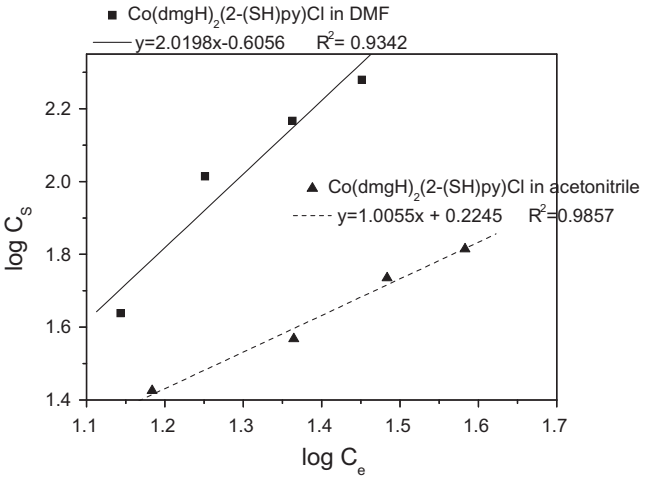

Fig. 2. Model fit of adsorption isotherm of $Co^{III}(dmgH)_2$(2-(SH)py)Cl 3 adsorbed on CdS in DMF and acetonitrile solutions.

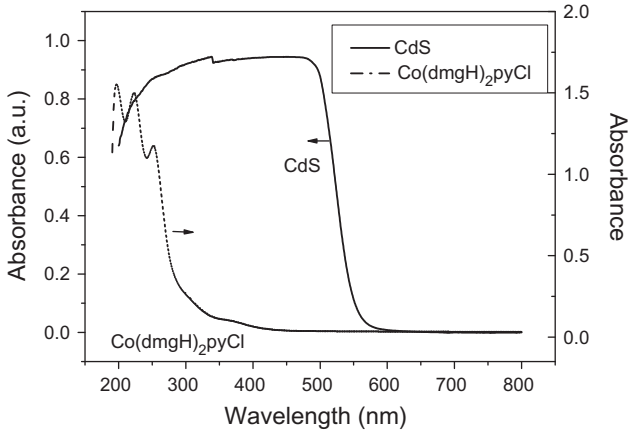

Fig. 3. UV–Vis diffuse reflectance spectrum of CdS and UV–Vis spectrum of $Co^{III}(dmgH)_2$pyCl in acetonitrile solution.

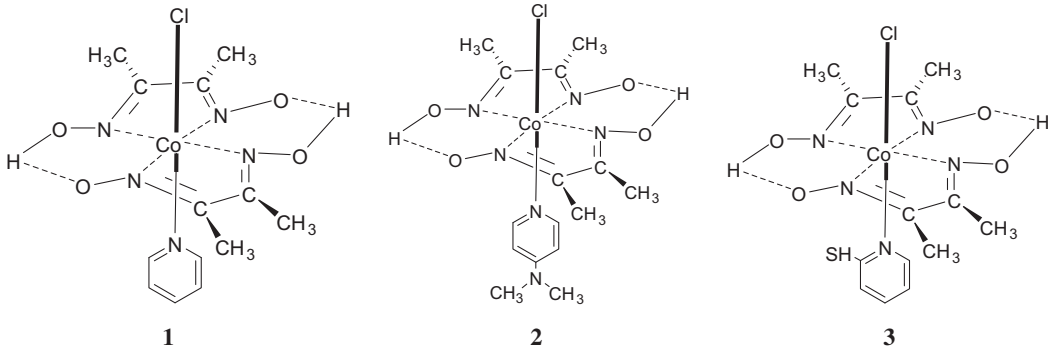

Fig. 1. Structure of different Co^{III} complexes: (**1**) $Co^{III}(dmgH)_2$pyCl. (**2**) $Co^{III}(dmgH)_2$(4-(Me_2N)py)Cl. (**3**) $Co^{III}(dmgH)_2$(2-(SH)py)Cl.

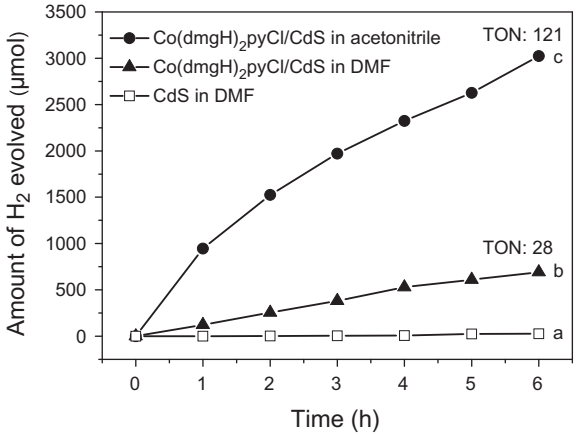

Fig. 4. Time courses of photocatalytic H_2 evolution over CdS and $Co(dmgH)_2pyCl$/CdS hybrid system in DMF solvent (line a and b) and in acetonitrile solvent (line c) under visible light irradiation ($\lambda > 420$ nm). CdS (0.05 g); $Co(dmgH)_2pyCl$ (0.25 mM); 10 vol.% TEOA (total solution volume 100 mL, 0.75 M); 10 vol.% H_2O (total solution volume 100 mL); 80 vol.% DMF or acetonitrile (total solution volume 100 mL); light source, Xe lamp (300 W).

constants for H_2O is 78.5) and also promote the proton transfer [42]. Moreover, a part of protons may come from H_2O [42]. **1**/CdS hybrid system shows relatively high stability as evidenced by no evident decay of photocatalytic activity in 6 h of irradiation. To clarify the important role of **1** played in the photocatalytic reactions, more experiments with different combinations were performed. As shown in Table 1, no H_2 is detected when TEOA is absent, suggesting that if the oxidation half-reaction doesn't work, the reduction half-reaction also doesn't work. When CdS is absent, **1** alone shows no photocatalytic activity, indicating that CdS plays the crucial role in light harvesting for photocatalysis. When other Co^{III} complexes such as **2** [21] and **3** [39] whose structures are similar to **1** are combined with CdS, high photocatalytic activity for H_2 evolution can be also obtained (Table 2). This implies that the hybrid photocatalytic system composed of semiconductor nanoparticles and cobaloximes catalysts is a general and efficient photocatalyst for H_2 evolution. The high efficiency of photocatalytic H_2 evolution catalyzed by the cobaloximes/CdS hybrid system is mainly due to the efficient electron transfer from CdS to cobaloximes on which proton is reduced to H_2.

The direction of charge transfer between CdS and **1** can be predicted according to the energy band structure of CdS and the redox potential of the metal complex. The conduction band potential of CdS is −0.9 V vs. NHE (pH = 7) [43], while the second reduction potential of Co(II) to Co(I) is −0.78 V vs. NHE for complex **1** (Table 2). This implies that electron transfer from CdS to **1** is thermodynamically favorable, which is responsible for the increase in the cathodic current when **1** is added (Fig. S4). The electron transfer from CdS to complex **2** or **3** is also thermodynamically favorable. There is no significant change in the potentials for the Co(II)/Co(I) couple between complexes **1–3** in which the axial pyridine ligand is replaced by 4-NMe_2 or 2-SH pyridine. Interestingly, however, these three complexes, **1–3**, exhibit different activities for hydrogen production, as shown in Table 2. Complex **2** with the more electron-donating pyridine (4-Me_2N-py) is more active than complex **1**, which is similar as the trend in electrocatalysis observed by Razavet et al. [21]. Complex **3** with thiol (–SH) substituted pyridine shows the highest activity among these three complexes. The best adsorption of complex **3** on CdS may be the main reason for its highest activity.

Besides the formation of Co(I), the reduction in **1** may lead to the formation of Co^0 colloids, which could act as hydrogen evolution cocatalyst or hydrogen evolution center [30]. In order to rule out the formation of Co^0 on the surface of CdS, TEM and EDX characterizations (Fig. 5) were carried out to examine the surface of CdS after a photocatalytic H_2 evolution reaction for 6 h in DMF solution. TEM image shows smooth CdS crystals without other particles deposited on them. EDX result further confirms the absence of Co species on the surface of CdS. Furthermore, UV–Vis spectra of solutions before and after photocatalytic reaction (Fig. S5) show that the complex **1** still remains intact in solution after irradiation of 6 h [21]. However, as time goes on, a gradual decomposition of **1** was found, as shown in Fig. 6. H_2 evolution is ceased after irradiation for 15 h with a TON of 171. The re-addition of same amount of **1** as first run (25 μmol) cause an almost totally recovered activity for H_2 evolution, while the re-adding of CdS could not regenerate H_2 under irradiation. These results indicate that deactivation of the system is mainly due to the decomposition of the Co complex and that the CdS is still active. The instability of $Co^{III}(dmgH)_2pyCl$ is mainly caused by the decomposition of dmgH ligand as reported by McCormick et al. [26]. It also suggests that the coordinated dmgH ligand is labile and undergoes exchange with free dmgH in solution. Therefore, the addition of extra dmgH can effectively improve the stability of Co^{III} complexes.

In order to know if a trace amount of Co^0 in solution may affect the photocatalytic H_2 evolution, $CoCl_2$, which can be reduced to Co^0 by photo-generated electrons of CdS (φ^0 for Co^0/Co^{2+} is −0.277 V vs. NHE), was tested for photocatalytic H_2 evolution under the same experimental conditions. The results show that the photocatalytic activity of Co/CdS is fairly lower than $Co^{III}(dmgH)_2pyCl$/CdS system (Table 3). This indicates that the high photocatalytic H_2 evolution activity of $Co^{III}(dmgH)_2pyCl$/CdS system can be only attributed to the efficient electron transfer from CdS to $Co^{III}(dmgH)_2pyCl$ where H^+ is reduced to H_2. In fact, we found that the photocatalytic activity of $Co^{III}(dmgH)_2pyCl$/CdS is even higher than that of Pt/CdS catalyst, which has been considered as a highly active photocatalyst for H_2 evolution (as shown in Table 3).

TEOA is widely used as a sacrificial electron donor in homogeneous photocatalytic H_2 evolution reactions [28–31], where TEOA can be oxidized by photo-generated holes (h^+) on photosensitizers to form $TEOA^+$ [44]. Here, in our work, TEOA is also oxidized by the photo-generated holes (h^+) on CdS. On the other hand, $Co^{III}(dmgH)_2pyCl$ is reduced by photo-exited electrons (e^-) on CdS to form Co(I) species. Considering the short lifetime of the exited state of CdS (nanosecond), one may wonder how this diffusion controlled reaction can take place. The existence of sacrificial electron donor makes it possible. Long-lived electrons (microsecond to second) can be produced by semiconductor when it is exposed to sacrificial electron donor [42,45,46]. This time scale is long enough to allow the reaction happen. The Co(I) species can be protonated to form Co(III)-H species followed by the release of H_2 through either mono- [28,30] or bimetallic catalysis pathway [21–23]. For the mono-Co mechanisms, the rate constant should have a linear dependence on [Co], whereas for the bimetallic mechanism, the rate should vary as $[Co]^2$. The results in Fig. 7 clearly show a

Table 1
Rate of photocatalytic H_2 evolution over different photocatalytic systems.

Photocatalytic systems	H_2 evolution rate (μmol h^{-1})[a]
$Co(dmgH)_2pyCl$/CdS in solution without TEOA	0.0
$Co(dmgH)_2pyCl$ in TEOA solution	0.0
CdS in TEOA solution	4.4
$Co(dmgH)_2pyCl$/CdS in TEOA solution	115.0

[a] Experiments were done under visible light irradiation ($\lambda > 420$ nm). CdS (0.05 g); $Co(dmgH)_2pyCl$ (0.25 mM); 10 vol.% TEOA (total solution volume 100 mL, 0.75 M); 10 vol.% H_2O (total solution volume 100 mL); 80 vol.% DMF (total solution volume 100 mL); light source, Xe lamp (300 W); irradiation time, 6 h.

Table 2
Electrochemical potentials[a] (V vs. NHE) for Co^{III} complexes and rate of photocatalytic H_2 evolution when combined with CdS.[b]

Co^{III} complex	Reduction $E(Co^{III}/Co^{II})$ (V)	Reduction $E_{1/2}(Co^{II}/Co^{I})$ (V)	H_2 evolution rate ($\mu mol\ h^{-1}$)[b]
1	−0.35	−0.78	46
2	−0.44	−0.79	77
3	−0.48	−0.80	100

[a] Cyclic voltammograms were obtained in degassed solution with 0.1 M nBu_4NPF_6 as supporting electrolyte at room temperature in DMF; scan rate: 100 mV/s; potential vs. NHE converted from internal standard Fc^+/Fc.

[b] Rate of photocatalytic H_2 evolution under visible light ($\lambda > 420$ nm). CdS (0.1 g); Co complexes (1.0 mM); 10 vol.% lactic acid (total solution volume 100 mL); 10 vol.% H_2O (total solution volume 100 mL); 80 vol.% DMF (total solution volume 100 mL); light source, Xe lamp (300 W); irradiation time, 3 h.

linearization dependence on $[Co]^2_{total}$, which implies a bimetallic catalysis pathway. One possibility for H_2 evolution is through the reaction of two adsorbed Co^{III}–H. Moreover, considering the weak adsorption capacity of **1** on CdS, the desorption of Co^{III}–H is also favorable. Therefore, hydrogen evolution through the reaction of the two Co^{III}–Hs in the solution or between the adsorbed one and the one in the solution is also possible.

It was reported that Co(II) and Co(I) species can be detected by UV–Vis spectroscopy after photolysis [28,30,31]. However, in this work, we did not observe the typical absorbance bands at 440 nm for Co(II) and 550 nm for Co(I) after the photocatalytic reaction for 10 min or 6 h. This might be interpreted in terms of that the heterogeneous interfacial electron transfer from semiconductor particles to the solution is fast [47], or the lifetime of intermediate is too short to be detected by the static spectroscopic techniques.

4. Conclusion

Visible light driven H_2 evolution can be successfully achieved (TON up to 171 based on $Co^{III}(dmgH)_2pyCl$) using the hybrid

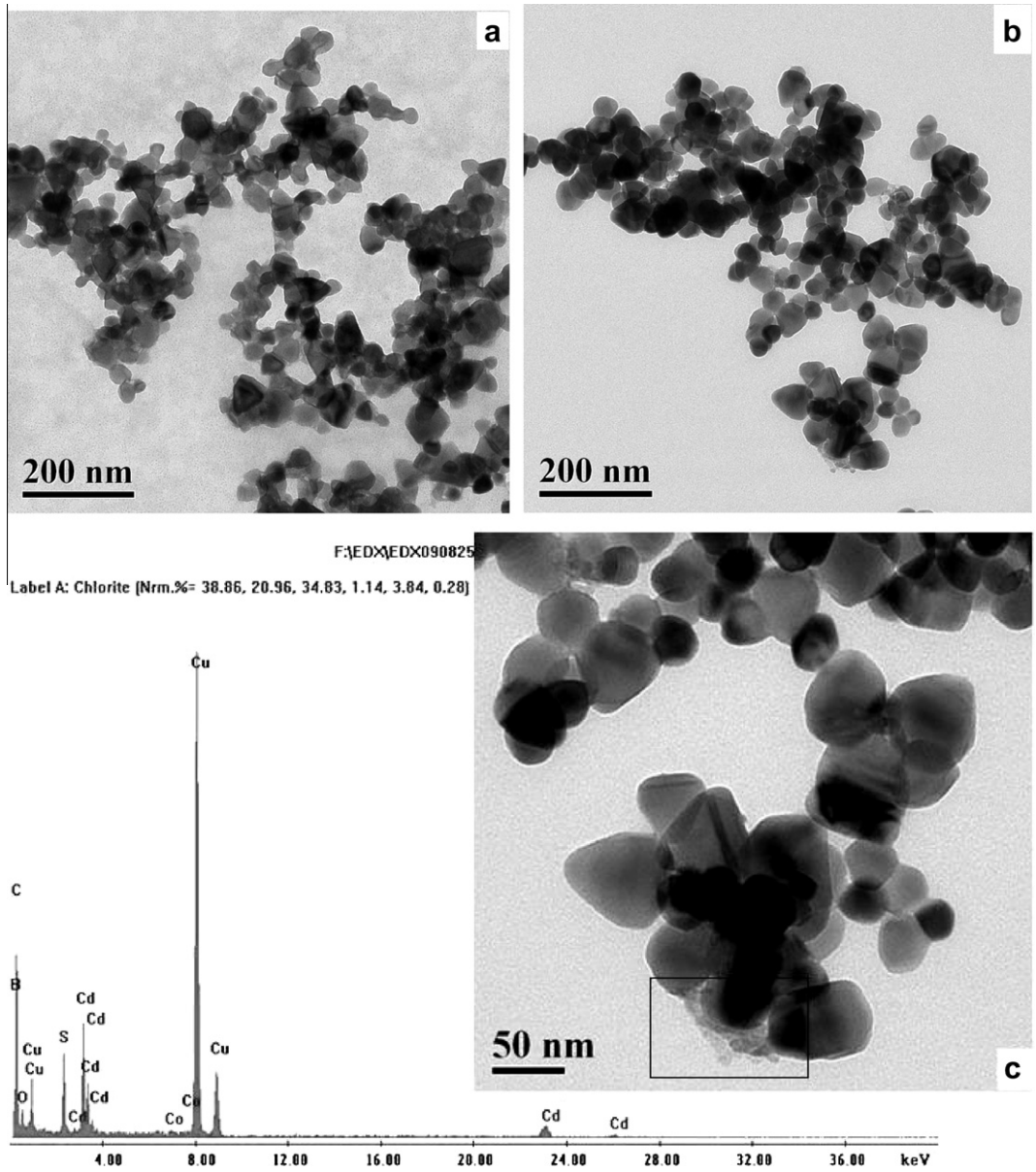

Fig. 5. TEM image of CdS: (a) before reaction; (b) after a reaction for 6 h in DMF solution; and (c) after a reaction for 6 h (enlarged) and EDX result of CdS after a reaction for 6 h in DMF solution.

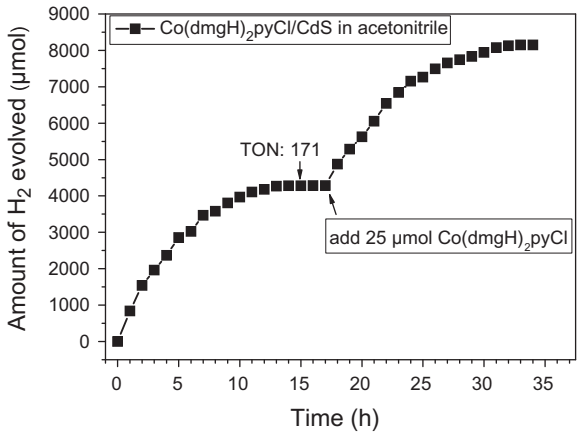

Fig. 6. Time courses of photocatalytic H_2 evolution over $Co(dmgH)_2pyCl/CdS$ in acetonitrile solvent showing the stability of the system with re-adding of $Co(dmgH)_2pyCl$ (25 μmol) to the system after irradiation of 17 h. Experiments were done under visible light irradiation ($\lambda > 420$ nm). CdS (0.05 g); $Co(dmgH)_2pyCl$ (0.25 mM); 10 vol.% TEOA (total solution volume 100 mL, 0.75 M); 10 vol.% H_2O (total solution volume 100 mL); 80 vol.% acetonitrile (total solution volume 100 mL); light source, Xe lamp (300 W).

Table 3
Rate and QE of photocatalytic H_2 evolution over different photocatalysts.

Photocatalysts	H_2 evolution rate (μmol h^{-1})[a]	QE (%)
CdS	4.4	0.08
Co/CdS	13.7	0.25
0.1 wt.% Pt/CdS	36.9	0.67
$Co(dmgH)_2pyCl/CdS$	115.0	2.1

[a] Experiments were done under visible light irradiation ($\lambda > 420$ nm). The loading of Pt and Co on CdS to produce Pt/CdS and Co/CdS was done by photodeposition of $CoCl_2$ and K_2PtCl_4. CdS (0.05 g); $Co(dmgH)_2pyCl$ (0.25 mM); $CoCl_2$ (0.25 mM); 10 vol.% TEOA (total solution volume 100 mL, 0.75 M); 10 vol.% H_2O (total solution volume 100 mL); 80 vol.% DMF (total solution volume 100 mL); light source, Xe lamp (300 W); irradiation time, 6 h.

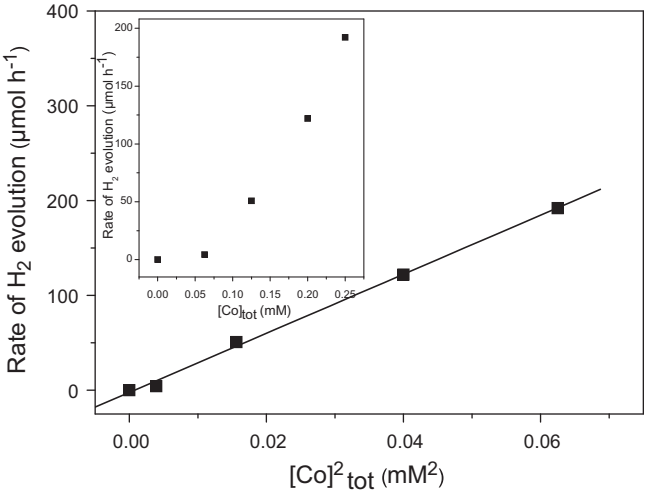

Fig. 7. Initial H_2 evolution rates as a function of $[Co]^2_{total}$ (inset: initial H_2 evolution rates as a function of $[Co]_{total}$). Experiments were done under visible light irradiation ($\lambda > 420$ nm). CdS (0.1 g); 10 vol.% TEOA (total solution volume 100 mL, 0.75 M); 10 vol.% H_2O (total solution volume 100 mL); 80 vol.% DMF (total solution volume 100 mL); light source, Xe lamp (300 W); irradiation time, 1 h.

photocatalytic system, which is composed of semiconductor CdS as photosensitizer and Co^{III} complexes as H_2 evolution catalysts. The efficient interfacial electron transfer from photoexcited CdS to Co^{III} complexes, the broad electronic absorption of photosensitizer CdS, together with the high catalytic H_2 producing activity of Co^{III} complexes are found to be responsible for the high photocatalytic activity of this hybrid system. This system bridges the gap between homogeneous and heterogeneous photocatalysis, and this strategy can be further extended to various hybrid systems containing semiconductors and H_2 evolution catalysts.

Acknowledgments

This work was financially supported by the National Basic Research Program of China (Grant No. 2009CB220010), the National Natural Science Foundation of China (NSFC, Grant Nos. 21090341, 21061140361), the Programme Strategic Scientific Alliances between China and the Netherlands (Grant No. 2008DFB50130) and Solar Energy Action Project of Chinese Academy of Sciences (Grant No. KGCX2-YW-391). The authors thank Dr. Hongxian Han for English revision and helpful suggestions.

Appendix A. Supplementary material

Supplementary data associated with this article can be found, in the online version, at doi:10.1016/j.jcat.2011.05.015.

References

[1] J. Barber, Chem. Soc. Rev. 38 (2009) 185.
[2] D. Gust, T.A. Moore, A.L. Moore, Acc. Chem. Res. 42 (2009) 1890.
[3] C. Tard, X.M. Liu, S.K. Ibrahim, M. Bruschi, L. De Gioia, S.C. Davies, X. Yang, L.S. Wang, G. Sawers, C.J. Pickett, Nature 433 (2005) 610.
[4] R. Mejia-Rodriguez, D.S. Chong, J.H. Reibenspies, M.P. Soriaga, M.Y. Darensbourg, J. Am. Chem. Soc. 126 (2004) 12004.
[5] L.C. Sun, B. Akermark, S. Ott, Coordin. Chem. Rev. 249 (2005) 1653.
[6] F. Gloaguen, T.B. Rauchfuss, Chem. Soc. Rev. 38 (2009) 100.
[7] F. Gloaguen, J.D. Lawrence, T.B. Rauchfuss, J. Am. Chem. Soc. 123 (2001) 9476.
[8] S. Ott, M. Kritikos, B. Akermark, L.C. Sun, R. Lomoth, Angew. Chem. – Int. Edit. 43 (2004) 1006.
[9] G.A.N. Felton, A.K. Vannucci, J.Z. Chen, L.T. Lockett, N. Okumura, B.J. Petro, U.I. Zakai, D.H. Evans, R.S. Glass, D.L. Lichtenberger, J. Am. Chem. Soc. 129 (2007) 12521.
[10] S. Ott, M. Kritikos, B. Akermark, L.C. Sun, Angew. Chem. – Int. Edit. 42 (2003) 3285.
[11] S. Ott, M. Borgstrom, M. Kritikos, R. Lomoth, J. Bergquist, B. Akermark, L. Hammarstrom, L.C. Sun, Inorg. Chem. 43 (2004) 4683.
[12] X. Zong, Y. Na, F.Y. Wen, G.J. Ma, J.H. Yang, D.G. Wang, Y. Ma, M. Wang, L. Sun, C. Li, Chem. Commun. (2009) 4536.
[13] Y. Na, J.X. Pan, M. Wang, L.C. Sun, Inorg. Chem. 46 (2007) 3813.
[14] Y. Na, M. Wang, J.X. Pan, P. Zhang, B. Akermark, L.C. Sun, Inorg. Chem. 47 (2008) 2805.
[15] P. Zhang, M. Wang, C.X. Li, X.Q. Li, J.F. Dong, L.C. Sun, Chem. Commun. 46 (2010) 8806.
[16] C. Li, M. Wang, J.X. Pan, P. Zhang, R. Zhang, L.C. Sun, J. Organomet. Chem. 694 (2009) 2814.
[17] J.L. Dempsey, B.S. Brunschwig, J.R. Winkler, H.B. Gray, Acc. Chem. Res. 42 (2009) 1995.
[18] G.M. Brown, B.S. Brunschwig, C. Creutz, J.F. Endicott, N. Sutin, J. Am. Chem. Soc. 101 (1979) 1298.
[19] P. Connolly, J.H. Espenson, Inorg. Chem. 25 (1986) 2684.
[20] R.M. Kellett, T.G. Spiro, Inorg. Chem. 24 (1985) 2373.
[21] M. Razavet, V. Artero, M. Fontecave, Inorg. Chem. 44 (2005) 4786.
[22] C. Baffert, V. Artero, M. Fontecave, Inorg. Chem. 46 (2007) 1817.
[23] X.L. Hu, B.S. Brunschwig, J.C. Peters, J. Am. Chem. Soc. 129 (2007) 8988.
[24] A. Fihri, V. Artero, M. Razavet, C. Baffert, W. Leibl, M. Fontecave, Angew. Chem. – Int. Edit. 47 (2008) 564.
[25] A. Fihri, V. Artero, A. Pereira, M. Fontecave, Dalton Trans. 1 (2008) 5567.
[26] T.M. McCormick, B.D. Calitree, A. Orchard, N.D. Kraut, F.V. Bright, M.R. Detty, R. Eisenberg, J. Am. Chem. Soc. 132 (2010) 15480.
[27] B. Probst, A. Rodenberg, M. Guttentag, P. Hamm, R. Alberto, Inorg. Chem. 49 (2010) 6453.
[28] P.W. Du, K. Knowles, R. Eisenberg, J. Am. Chem. Soc. 130 (2008) 12576.
[29] B. Probst, C. Kolano, P. Hamm, R. Alberto, Inorg. Chem. 48 (2009) 1836.
[30] P.W. Du, J. Schneider, G.G. Luo, W.W. Brennessel, R. Eisenberg, Inorg. Chem. 48 (2009) 4952.
[31] T. Lazarides, T. McCormick, P.W. Du, G.G. Luo, B. Lindley, R. Eisenberg, J. Am. Chem. Soc. 131 (2009) 9192.
[32] A. Kudo, Y. Miseki, Chem. Soc. Rev. 38 (2009) 253.

[33] K. Maeda, K. Teramura, D. Lu, T. Takata, N. Saito, Y. Inoue, K. Domen, Nature 440 (2006) 295.
[34] K. Maeda, K. Domen, J. Phys. Chem. C 111 (2007) 7851.
[35] X. Zong, H. Yan, G. Wu, G. Ma, F. Wen, L. Wang, C. Li, J. Am. Chem. Soc. 130 (2008) 7176.
[36] H. Yan, J. Yang, G. Ma, G. Wu, X. Zong, Z. Lei, J. Shi, C. Li, J. Catal. 266 (2009) 165.
[37] T. Nann, S.K. Ibrahim, P.M. Woi, S. Xu, J. Ziegler, C.J. Pickett, Angew. Chem. – Int. Edit. 49 (2010) 1574.
[38] G.N. Schrauzer, Inorg. Synth. 11 (1968) 61.
[39] Y. Gok, S.Z. Yildiz, Synth. React. Inorg. Met. – Org. Chem. 22 (1992) 1327.
[40] Y. Wan, Y.Y. Bao, Q.X. Zhou, Chemosphere 80 (2010) 807.
[41] J. Lee, H.H. Seliger, J. Chem. Phys. 40 (1964) 519.
[42] T. Chen, Z.H. Feng, G.P. Wu, J.Y. Shi, G.J. Ma, P.L. Ying, C. Li, J. Phys. Chem. C 111 (2007) 8005.
[43] K. Kalyanasundaram, E. Borgarello, M. Gratzel, Helv. Chim. Acta 64 (1981) 362.
[44] K. Kalyanasundaram, J. Kiwi, M. Gratzel, Helv. Chim. Acta 61 (1978) 2720.
[45] A. Yamakata, T. Ishibashi, H. Onishi, J. Phys. Chem. B 106 (2002) 9122.
[46] A. Yamakata, T.A. Ishibashi, J. Onishi, J. Phys. Chem. B 107 (2003) 9820.
[47] A. Boulesbaa, A. Issac, D. Stockwell, Z. Huang, J. Huang, J. Guo, T. Lian, J. Am. Chem. Soc. 129 (2007) 15132.